

Electronic screening and correlated superconductivity in carbon nanotubes

S. Bellucci¹, M. Cini^{1,2}, P. Onorato^{1,3} and E. Perfetto⁴

¹INFN, Laboratori Nazionali di Frascati, P.O. Box 13, 00044 Frascati, Italy

²Dipartimento di Fisica, Università di Roma Tor Vergata,

Via della Ricerca Scientifica 1 00133, Roma, Italy

³Department of Physics "A. Volta", University of Pavia, Via Bassi 6, I-27100 Pavia, Italy

⁴Consorzio Nazionale Interuniversitario per Le Scienze Fisiche della Materia,

Università di Roma Tor Vergata, Via della Ricerca Scientifica 1 00133, Roma, Italy

(Dated: September 16, 2018)

A theoretical analysis of the superconductivity observed recently in Carbon nanotubes is proposed. We argue that ultra-small (diameter $\sim 0.4\text{nm}$) single wall carbon nanotubes (with transition temperature $T_c \sim 15\text{ }^{\circ}\text{K}$) and entirely end-bonded multi-walled ones ($T_c \sim 12\text{ }^{\circ}\text{K}$) can superconduct by an electronic mechanism, basically the same in both cases. By a Luttinger liquid -like approach, one finds enhanced superconducting correlations due to the strong screening of the long-range part of the Coulomb repulsion. Based on this finding, we perform a detailed analysis on the resulting Hubbard-like model, and calculate transition temperatures of the same order of magnitude as the measured ones.

I. INTRODUCTION

Carbon nanotubes as one-dimensional (1D) molecular conductors are among the best candidates for investigating the possibility of 1D superconductivity. They are basically rolled up sheets of graphene forming tubes that are only nanometers in diameter and length up to some microns. Carbon nanotubes may be grown as single-walled (SWNT) or multi-walled (MWNTs), that are typically made of several coaxial graphene shells. They show semi-conducting or metallic properties depending on the helicity of the carbon rings around the tubule¹.

The electron-electron interactions are also known to modify significantly the transport properties of the nanotubes², leading to the breakdown of the conventional Fermi liquid picture. In fact the 1D character of the system leads to a strong correlation among electrons, inducing of the so-called Luttinger liquid³. The Luttinger liquid behavior is characterized by a power-law suppression of physical observables, such as the tunnelling conductance, over a wide range of temperatures. Indeed the tunneling conductance G reflects the power law dependence of the tunneling density of states (DOS), in a small bias experiment⁴

$$G = dI/dV \propto T^\alpha \quad (1)$$

for $eV \ll kT$, where V is the bias voltage, T is the temperature and k is Boltzmann's constant. Evidence of Luttinger liquid behavior in SWNTs has been found in many experiments^{5,6,7}, where the temperature dependence of the resistance above a crossover temperature T_c was measured⁸. The critical exponent α assumes different values for an electrode-bulk junction (α_{bulk}) and for an electrode-end junction (α_{end}), as reported for MWNTs in Ref.9.

Experiments have been also carried out to show superconducting correlations in SWNTs at low temperatures. Clear evidence of superconductivity was found in nanotubes suspended between superconducting contacts,

showing the so-called proximity effect^{10,11}. Moreover, genuine superconducting transitions below 1K have been observed in thick ropes of nanotubes suspended between normal and highly transparent electrodes¹².

A few years ago, ultra-small-diameter single wall nanotubes (USCN), with diameter of $\sim 0.4\text{ nm}$, have been produced inside the channels of a zeolite matrix. Possible metallic geometries compatible with such a small radius are the armchair (3,3) and the zig-zag (5,0) ones. The ultra-small diameter of these tubes induces many unusual properties, such as a superconducting transition temperature $T_c \approx 15\text{K}$ ¹³, much larger than that observed in bundles of larger diameter tubes¹⁴.

Quite recently¹⁵ a similar transition temperature was observed in entirely end-bonded MWNTs. It was found that the emergence of superconductivity ($T_c = 12\text{K}$) is highly sensitive to the junction structures of the Au electrode/MWNTs.

The question arises, whether the superconductivity in the MWNTs¹⁵ can be understood on the same grounds as the superconductivity of the USNTs¹⁶. Here, we argue that a purely electronic mechanism could work in both cases. We start by a Tomonaga-Luttinger model of the electronic system, focussing on the most relevant sources of screening of the Coulomb repulsion. The long-range part of the interaction can be strongly reduced due to the peculiarity of the experimental conditions. This opens up the possibility of a breakdown of the Luttinger liquid regime towards a pairing instability. Anyway this finding calls for a more detailed analysis based on an effective Hubbard model, emphasizing the role of the short range interaction. We have in mind a basically electronic mechanism, but lattice effects should be considered as well. The analysis could be carried out along the lines of Ref.¹⁷, where the interplay of phonons with the W=0 mechanism was discussed. Since this is very demanding in the present geometry the problem is deferred to future publications.

II. LUTTINGER LIQUID IN CARBON NANOTUBES

The Luttinger liquid is the prototype of interacting electrons in 1D and it is governed by the so called Tomonaga-Luttinger Hamiltonian. In this model, the electrons have linear dispersion relation around positive (Right) and negative (Left) Fermi points located at $\pm K_F$ and the e-e interactions act only between Right or Left electron densities. This means that only the *forward scattering* component with small momentum transfer $q \sim 2\pi/L \equiv q_c$ of the Coulomb repulsion (denoted by g_2) is retained, while the *backscattering* component with $q \sim 2K_F$ (denoted by g_1) is assumed to be negligible. Anyway, even a small g_1 is important at low temperatures since it may induce the breakdown of the Luttinger liquid state toward a phase transition.

In normal conditions, a carbon nanotube is composed itself by two coupled (identical) Luttinger liquids, since there are a Left and a Right linear branch respectively around each of the two Fermi points at $(\pm K_F, 0)$ ($K_F = 4\pi/3a$, and $a = 2.46\text{\AA}$ is the lattice constant). These branches are highly linear with Fermi velocity $v_F \approx 8 \times 10^5 \text{ m/s}$. The linear dispersion relation holds for energy scales $E < D$, with the bandwidth cutoff scale $D \approx \hbar v_F/R$ for tube radius R .

In order to study the effects of interactions, we introduce the unscreened Coulomb repulsion in a wrapped 2D geometry

$$V_0(x - x', y - y') = \frac{e^2/\kappa}{\sqrt{(x - x')^2 + 4R^2 \sin^2(\frac{y - y'}{2R})}}, \quad (2)$$

where x denotes the coordinate along the tube axis and $0 < y < 2\pi R$ is the coordinate along the circumference of the transverse cross-section of the tube. The Fourier transform $\hat{V}_0(q)$ reads

$$\hat{V}_0(q) \approx \frac{e^2/\kappa}{\sqrt{2}} \left[K_0\left(\frac{qR}{2}\right) I_0\left(\frac{qR}{2}\right) \right], \quad (3)$$

where κ is the dielectric constant, $K_0(q)$ denotes the modified Bessel function of the second kind, $I_0(q)$ is the modified Bessel function of the first kind. The nanotube radius R yields a natural cutoff $\approx \frac{2\pi}{R}$ of the interaction.

According to the above discussion we have $g_2 = \hat{V}_0(q_c)$ and $g_1 = \hat{V}_0(2K_F)$. Following Ref.3, we introduce an additional interaction (f) which measures the difference between intra- and inter-sublattice interactions. Such a term is not contained in Eq.(3) and it is due to the hard core of the Coulomb interaction.

The Luttinger liquid behavior in carbon nanotubes was theoretically investigated in Ref.3, where the low-energy theory including Coulomb interaction is derived. Although the analysis is quite general, explicit results were obtained for typical metallic nanotubes, i.e. armchair $(10, 10)$ SWNTs with radius $R \approx 1.4\text{nm}$ and length $L \approx 3\mu\text{m}$, which we name CN_{10} .

The Luttinger parameter g depends just on the forward scattering part of the interaction

$$\frac{1}{g} = \sqrt{1 + \frac{g_2}{(2\pi v_F)}}, \quad (4)$$

whereas the critical exponent can be written in terms of g as $\alpha_{bulk} = \frac{1}{4}(g + 1/g - 2)$. A detailed estimate for the CN_{10} gives $g \approx 0.2$ and $\alpha_{bulk} \approx 0.32$, in agreement with experiments³.

Concerning the rest of the couplings, it is shown that both g_1 and f scale as $1/R$ and in CN_{10} they are much smaller than g_2 ³. Anyway at low temperature their effects should be included. In Ref.3 this has been realized by means of a renormalization group calculation.

The main result is the existence of two different crossover temperatures, namely $kT_f = De^{-\frac{2\pi v_F}{f}}$ and $kT_b = De^{-\frac{2\pi v_F}{g_1}}$ associated to the dominance of f and g_1 respectively. Below these temperatures the Luttinger liquid breaks down and a (quasi-) long-range order phase appears. For long-ranged interactions (which is the case of nanotubes in typical conditions), we have $T_f \sim T_b$, while for short-ranged interactions it results $T_f < T_b$. In the latter case a superconducting instability is predicted at $T \sim T_f$ if the Luttinger liquid parameter g is larger than $1/2$. This condition implies a very strong screening of g_2 and it is the main aim of the present paper to show that such an instance can be realized in the experimental conditions of Refs.13 and 15.

Anyway it is worth to note that the transition temperature for CN_{10} with the typical long-range interaction as in Eq.(2) is estimated to be $T_f \sim T_b \sim 1\text{mK}$, i.e. a value certainly hard to be observed. This is due to the smallness of g_1 and f (compared to g_2), since they scale as $1/R$ and are sizeable only for very thin tubes.

Starting from the results of Ref.3 it appears that a pure electronic mechanism consistent with an observable superconductivity in the nanotubes requires a strong reduction of the forward scattering g_2 (so that $g > 1/2$) and the increase of g_1 and f with respect to the values of typical samples.

III. ULTRA SMALL NANOTUBES

In this Section we analyze the screening properties of ultra small nanotubes, due to the experimental setup of Ref.13. In particular we show that the presence of many nanotubes inside the zeolite matrix provides a strong screening of the long range component of the electron-electron interaction (g_2), while the short range components have to remain almost unchanged. This allows for the occurrence of a sizable superconducting instability within the Luttinger liquid approach. In what follows we focus on the $(3,3)$ nanotubes as the main candidate to be present inside the zeolite matrix (we shall refer to them as CN_3), although the possibility of a presence of $(5,0)$ zig-zag tubes cannot be discarded.

As already pointed out in Refs.18 and 19, the intra-tube Coulomb repulsion at small momentum transfer (i.e. in the forward scattering channel) is efficiently screened by the presence of electronic currents in neighboring nanotubes. In the experimental samples of Ref.13 the carbon nanotubes are arranged in large arrays with triangular geometry, behaving as a genuine 3D system. By means of a generalized Random Phase Approximation (RPA) approach, it is shown^{18,19} that the forward scattering parameter g_2 gets renormalized according to

$$g_2^{CN_3} \rightarrow (\hat{U})_{s,s}, \quad (5)$$

where $(\hat{U})_{s,s'}$ obeys to the Dyson equation

$$(\hat{U})_{s,s'} = [\hat{U}_0(1 - \hat{U}_0\Pi_0)^{-1}]_{s,s'} \quad (6)$$

where $\Pi_0 = 1/2\pi v_F$ and the matrix $(\hat{U}_0)_{s,s'}$ is given by

$$(\hat{U}_0)_{s,s'} = \frac{1}{3^2} \int_0^L dx \sum_{y,y'} U_0(x, y, y', s, s'), \quad (7)$$

Here $U_0(x, y, y', s, s')$ is the 3D bare Coulomb repulsion between two electrons in (3,3) nanotubes in the zeolite matrix such that x is the relative coordinate in the longitudinal direction, s, s' indicate the position of the two nanotube axes in the zeolite matrix and y, y' are the circular coordinates in each nanotube. We note that if $s = s'$ we recover $U_0(x, y, y', s, s) = V_0$ as in Eq.(2).

The above source of screening provides $g_2^{CN_3}/v_F = (\hat{U})_{s,s}/v_F \approx 0.7$ (see Fig.5 of Ref.19), where it is used that the distance between nearest neighbors nanotubes in the matrix is 1nm. This result indicates a large reduction (by a factor $\approx 10^{-2}$) with respect to the bare coupling. The backscattering coupling g_1 is not affected appreciably.

Let us analyze now how the couplings g_1 and f are modified in USNTs. As shown in Ref.3, they scale as $1/R$ and therefore are $10/3$ times larger in the CN_3 than in the CN_{10} . The additional forward scattering f corresponds to³ $\delta V_p = V_{++} - V_{+-}$, where $V_{p,p'}$ is the interaction between electrons belonging to different sublattices (p, p'), and it is strongly suppressed at a distance much larger than $\ell \sim 0.3\text{nm}^{16}$. In the same way, the only non-vanishing contribution to g_1 comes from $|x - x'| \leq a$, because of rapidly oscillating contributions³.

As a consequence we find the relation $g_1^{CN_3} \sim \frac{10}{3}g_1^{CN_{10}}$ and the same also holds for f . All of the above mentioned effects have a strong impact on the crossover temperature T_c , and following ref.³ we estimate

$$kT_b \sim kT_f \sim kT_c \propto De^{-\frac{2\pi v_F}{g_1}}. \quad (8)$$

For the CN_{10} , T_c was estimated as $\sim 0.1\text{mK}$, or some order of magnitude larger for well-screened interaction³. It follows that in USNTs T_c should be several orders of magnitude larger than the one predicted for a CN_{10} with a factor compatible with the observed critical temperature.²⁰ To sum up, one can expect that the

screening of the short-range part of the Coulomb interaction be less efficient in CNTs than in bulk graphite; moreover, in CN_3 it will be less efficient than in CN_{10} . This is an unavoidable consequence of the reduced effective dimensionality, which puts constraints on the screening cloud. We wish to emphasize that the above arguments lead to the conclusion that the increased short range repulsion does not impair T_c , as one could naively expect; actually the critical temperature turns out to increase, at least for a moderate increase of the short-range component of the Coulomb repulsion. This seemingly paradoxical conclusion is further validated by a thorough analysis within the Hubbard model, as shown in the next subsection.

A. Hubbard model for ultra small nanotubes

The results of the previous Section suggest the possibility of a superconducting instability in USNTs within the Luttinger liquid scenario. Indeed lattice effects and very short range interactions become dominant so that the Luttinger liquid picture can break down at a sizable energy scale. Anyway we point out that, as long as g_1 and f become comparable to g_2 , all of them should be treated on the same footing. This indicates that the system under consideration should be better described in the Hubbard-like framework, which emphasizes the role of the lattice and the short range interaction. We recall that the Hubbard Hamiltonian reads:

$$H = H_0 + W = t \sum_{\langle \mathbf{r}, \mathbf{r}' \rangle} \sum_{\sigma} (c_{\mathbf{r},\sigma}^\dagger c_{\mathbf{r}',\sigma} + h.c.) + U \sum_{\mathbf{r}} n_{\mathbf{r},\uparrow} n_{\mathbf{r},\downarrow}, \quad (9)$$

where $c_{\mathbf{r},\sigma}^\dagger$ ($c_{\mathbf{r},\sigma}$) is the creation (annihilation) operator of a graphitic p_z electron of spin σ on the wrapped honeycomb lattice site \mathbf{r} , the sum runs over the pairs $\langle \mathbf{r}, \mathbf{r}' \rangle$ of nearest neighbour carbon atoms, $n_{\mathbf{r},\sigma} = c_{\mathbf{r},\sigma}^\dagger c_{\mathbf{r},\sigma}$ is the number operator referred to the site \mathbf{r} , t is the hopping parameter and U is the on-site Hubbard repulsion.

In Ref.21 the superconductivity in carbon nanotubes described by Eq.(9) was investigated with the renormalization group technique. Unfortunately this approach does not allow for a stringent prediction of the critical temperature.

In Ref.22 it was proposed an electronic mechanism which leads to superconducting pairing starting from the Hubbard model on the wrapped honeycomb lattice away from half filling. In this approach all the interaction channels are considered on the same footing and this makes it possible to predict a reliable transition temperature for the USNTs¹⁶.

The findings of Ref.22 are based on the so called $W = 0$ theory²³; this provides a singlet pairing mechanism operating on a lattice with Hubbard interaction and is otherwise somewhat analogue to the Kohn-Luttinger mechanism²⁴. On the basis of symmetry arguments, it is

possible to show that the Hamiltonian in Eq.(9) admits two-body singlet eigenstates with no double occupancy on the honeycomb sites, called $W = 0$ pairs. $W = 0$ pairs are therefore eigenstates of the kinetic energy operator H_0 and of the Hubbard repulsion W with vanishing eigenvalue of the latter. As a consequence the electrons forming a $W = 0$ pair have no direct interaction and are good candidates to achieve bound states. As a consequence the electrons forming a $W = 0$ pair have no direct interaction and are good candidates to achieve bound states. Their effective interaction V^{22} comes out from virtual electron-hole excitation exchange with the Fermi sea and in principle can be attractive²³. The binding energy Δ of the $W = 0$ pairs for an armchair (n, n) nanotube can be obtained by solving the gap equation

$$\frac{1}{V} = \frac{1}{8n} \frac{1}{2\pi} \sum_{k_y} \int dk_x \frac{\theta(\varepsilon(k_x, k_y) - \varepsilon_F)}{2(\varepsilon(k_x, k_y) - \varepsilon_F) - \Delta}, \quad (10)$$

where ε_F is the Fermi energy, $\varepsilon(k_x, k_y)$ is the eigenvalues of H_0 relative to momentum (k_x, k_y) (x is along the tube axis and y denotes the transverse direction). We recall that the effective interaction V between the two electrons forming the $W = 0$ pair encodes an indirect interaction mediated by the exchange of virtual electron-hole excitations. V is a complicated function of the Hubbard U , but does not contain any $o(U)$ contribution because of the $W = 0$ property²².

Remarkably it is found²² that Δ is nonvanishing only for the doped systems and increases with decreasing R and with increasing U , at least for moderate repulsion. Such a result confirms that in USNTs the superconducting phase is supported by the small size (i.e. larger Hubbard repulsion) in the presence of doping. Indeed, the $W = 0$ mechanism requires moving the Fermi level away from half filling. This can be achieved in several ways. CNTs can exchange charge with the surroundings by doping or by contact potential difference, due to the contacts with the zeolite matrix and/or the electrodes. The innermost nanotubes in multiwalled structures can conceivably exchange some charge with the outer ones. A shift of the order of 10^{-1} eV is sufficient to produce a sizable Δ in very small CNTs (see Fig. 5 in Ref.22). Note that it would be hard to ensure perfect neutrality of such tiny structures in inhomogeneous environments, so it is reasonable to assume that such a small shift in the Fermi level is easily realized.

Now, the first step in order to have a quantitative estimate of T_c in USNTs is a sensible evaluation of U . Because of the screening property due to the experimental conditions we find $g_2^{CN_3} \sim g_1^{CN_3} \sim f^{CN_3} \sim Ua/n$. Therefore $g_2^{CN_3}/v_F \approx 0.7$ implies $U \approx 0.7 \times 3 \times v_F/a \approx 4.2$ eV. In Ref.22 $U/t = 1.6$ was used (with $t = 2.6$ eV the hopping parameter of graphitic honeycomb lattice), which means $U = 4.4$ eV. This is reasonable in the light of other data available. In bulk Graphite, the Auger line shape analysis²⁶ gives a repulsion $U = 5.5$ eV between p holes. Therefore, the results of Ref.22 fairly ap-

ply to the case under consideration and we can extrapolate $\Delta \approx 8$ meV for (3,3) nanotubes at optimal doping. Finally, the BCS formula $\Delta = 1.76kT_c$ for the mean field transition temperature gives

$$T_c \approx 7 \div 70K$$

which is compatible with the measured one. We observe that the lower boundary $T_c \sim 7K$ takes into account that Δ may vary of about one order of magnitude away from optimal doping.

Finally we remark that the corresponding T_c for the CN_{10} is of the order of the mK in agreement with the predictions of Ref.3.

IV. ENTIRELY END-BONDED MWNTS

The experiment of Ref.15 has shown that "entirely end-bonded" MWNTs can superconduct at temperatures as high as 12 °K. In this system the authors claim that almost all the shells of the MWNT's are electrically active. Such a high quality of the contacts seems to be crucial, in order to observe the superconducting transition at such a high temperature.

Moreover the clear power-law of the conductance observed for $T > T_c$ is consistent with the Luttinger liquid character of the normal state. Therefore the observed sharp breakdown of the power-law at T_c is an indication that our approach based on the superconducting instability of the Luttinger liquid is well posed.

Now we discuss some relevant physical consequences of the activation of several shells. In a typical transport experiment, only the outermost shell of the MWNT becomes electrically active. As a consequence the conducting channel is not efficiently screened and retains a strong 1D character. On the other hand, the activation of the internal shells gives a large dielectric effect, due to intra- and inter-shell screening, and at the same time it provides an incipient 3D character, which is crucial for establishing the superconducting coherence.

We assume that all contacted shells can transport the normal current as resistors in parallel connection. Therefore at $T > T_c$, the electrons flow in each shell. It is however clear that the conductance G is mainly given by the outermost shells, because they have more conducting channels due to larger radius.

For what concerns $T < T_c$, we know from the previous Section that superconductivity is favored in the inner part of the MWNT, where the radius of the shells is reduced. In particular, we focus our attention on the innermost shell corresponding to a radius as small as $R_{in} \approx 0.4$ nm (e.g. a (6,6) armchair). We can wonder whether this shell can display a superconducting transition, and what is the corresponding T_c .

Following the discussion reported above we have to evaluate the screening of the long range interaction g_2 which determines the forward scattering coupling and the corresponding values of the short range terms g_1 and f .

As already discussed above, the g_2 interaction is screened by the electronic currents located in the surrounding (n, n) shells. A similar calculation as is Section III leads to the following renormalization of g_2 in a given shell n .

$$g_2^{CN_n} \rightarrow (\hat{W})_{n,n}, \quad (11)$$

where $(\hat{W})_{n,n'}$ obeys to the Dyson equation

$$(\hat{W})_{n,n'} = [\hat{W}_0(1 - \hat{W}_0\Pi_0)^{-1}]_{n,n'} \quad (12)$$

where the matrix $(\Pi_0)_{n,n'}$ reads

$$(\Pi_0)_{n,n'} = \sum_i \frac{1}{2\pi v_{F,n}(i)} \quad (13)$$

where the sum runs over all the Fermi points i (with related Fermi velocities $v_{F,n}(i)$) in the shell n . The matrix $(\hat{W}_0)_{n,n'}$ is given by

$$(\hat{W}_0)_{n,n'} = \frac{1}{nn'} \int_0^L dx \sum_{y,y'} W_0(x, y, y', n, n'), \quad (14)$$

Here $W_0(x, y, y', n, n')$ is the 3D bare Coulomb repulsion between two electrons in (n, n) and (n', n') shells, x is the relative coordinate in the longitudinal direction, y, y' are the circular coordinates in each shell. We note that also in this case we recover $W_0(x, y, y', n, n) = V_0$ as in Eq.(2).

For the innermost (6,6) shell, where superconducting correlations are expected to be enhanced, we find $g_2^{CN_6}/v_F = (\hat{W})_{6,6}/v_F \approx 0.5$, which again indicates a very strong screening. Here we used that the innermost shell has a radius $R_{in} \approx 0.4\text{nm}$, while the outermost shell has $R_{out} \approx 5\text{nm}$; this implies that the total number of shells in the MWNT is $N_{\text{shell}} \approx 15$ (we recall that the typical intershell distance is 0.34nm). Moreover we assumed, that because of doping, all the shells have a metallic character. We observe that the multiwalled geometry provides more efficient (alough of the same order) screening effect with respect to the array geometry.

Concerning the rescaling of g_1 and f , they scale as $1/R$, as we discussed above. In fact the short range component of the interaction is not affected appreciably by the surrounding conducting channels.

Thus the temperature T_c can be obtained from Eq.(8) by taking into account the modified values of g_1 and D as $T_c \sim 2 - 20K$, which corresponds to a transition temperature in the same range of values as the one observed for MWNTs.

A. Hubbard model for the innermost shell

At the light of the above discussion, we predict the presence of a superconducting instability in the innermost shell of the MWNTs of Ref.4, where the short-range

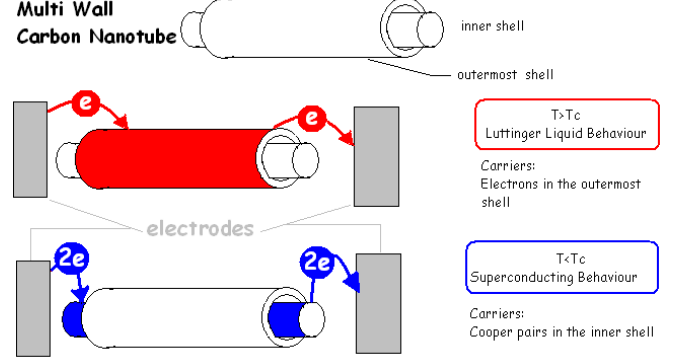


FIG. 1: We assume that all shells of an entirely end bonded MWNT are resistors in a parallel connection. For $T > T_c$ the current is due to the flow of electrons in the outermost shells with the typical behaviour of a Luttinger Liquid. For $T < T_c$ a superconducting transition is allowed in the innermost shell; thus the transport is due to Cooper pairs.

correlation effects become dominant. Again we have to give a sensible estimate for the Hubbard repulsion U .

The analysis of the screening properties of the experimental setup gives $g_2^{CN_6} \sim g_1^{CN_6} \sim f^{CN_6}$ for the innermost shell. Therefore $g_2^{CN_6}/v_F \approx 0.5$ implies $U \approx 0.5 \times 6 \times v_F/a \approx 6.0\text{eV}$. Therfore the results of Ref.25 can be applied, where $U/t = 2.5$ (and hence $U = 6.5\text{eV}$) was used. This is somewhat larger than the Graphite value²⁶. From that reference we find $\Delta \approx 5.5\text{meV}$ for (6,6) nanotubes at optimal doping, which means

$$T_c \approx 4 \div 40K.$$

This value is slightly lower than the one of USNTs, in qualitative agreement with the experimental findings. Also in this case the lower boundary $T_c \sim 4K$ is understood in terms of possible deviation from optimal doping.

Let us now comment upon the main result of this Section. In usual conditions, transport measurements carried out in MWNTs reflect the electronic properties of the outer shell, which the electrodes are attached to. On the other hand, in entirely end-bonded samples the inner shells are electrically active, with relevant consequences. In particular the innermost one is able to support the transport of Cooper pairs below a temperature consistent with the measured one.

V. CONCLUSIONS

Carbon nanotubes are not naturally superconducting. The main reason for this is the presence of a stable Luttinger liquid phase, as a reflection of the strong electron-electron repulsion, preventing Cooper pairs to form at sizable temperature.

Some recent experiments have shown that in particular conditions it is possible to observe superconducting cor-

rrelations, which can compete with the Luttinger liquid phase and even overcome it.

We propose a scenario where the Luttinger liquid can break down at sizable energy scales, assuming that (i) the radius of the tube is small enough, (ii) an efficient screening of the forward scattering interaction can be achieved. In these conditions a superconducting instability can arise by a purely electronic mechanism, and a model based on the Hubbard interaction predicts a crossover temperature T_c of the same order of magnitude as the measured one.

In USNTs of Ref.13, the presence of the many nanotubes in the surrounding zeolite matrix is quite relevant for the screening of the long range interaction, while the small size of the tubes is crucial, in order to increase the strength of the short range interactions g_1 and f . The

mechanism requires doping the nanotube away from half filling, but a shift of the Fermi energy by tens of an eV can produce a sizable Δ .

In the case of entirely end-bonded MWNTs, the screening of g_2 is due to the presence of many shells. Based on this consideration, we assume that all shells are resistors in a parallel connection. Therefore the current is mainly due to the flow of electrons in the outermost shells for $T > T_c$, i.e. in the Luttinger liquid phase, while the transport of Cooper pairs holds in the innermost and thinnest shell at $T < T_c$ (see Fig.1). This scenario is in line with the prediction^{22,25} of an increase in pair binding energy with decreasing nanotube radius.

E. P. was supported by INFN grant 10068. E. P. acknowledges Consorzio Nazionale Interuniversitario per Le Scienze Fisiche della Materia for financial support.

¹ N. Hamada, S. I. Sawada, and A. Oshiyama, Phys. Rev. Lett. **68**, 1579 (1992); R. Saito *et al.*, Appl. Phys. Lett. **60**, 2204 (1992).

² Z. Yao *et al.*, Nature **402**, 273 (1999).

³ R. Egger, and A. O. Gogolin, Phys. Rev. Lett. **79**, 5082 (1997); R. Egger, and A. O. Gogolin, Eur. Phys. J. B **3**, 281 (1998).

⁴ C. L. Kane, and M. P. A. Fisher, Phys. Rev. B **46**, 15233 (1992); C. L. Kane, and M. P. A. Fisher, Phys. Rev. Lett. **68**, 1220 (1992).

⁵ Z. Yao, H. W. Postma, L. Balents, and C. Dekker, Nature London **402**, 273 (1999).

⁶ C. Kane, L. Balents, and M. P. A. Fisher, Phys. Rev. Lett. **79**, 5086 (1997).

⁷ M. Bockrath, D. H. Cobden, J. Lu, A. G. Rinzler, R. E. Smalley, L. Balents, and P. L. McEuen, Nature **397**, 598 (1999).

⁸ J. E. Fischer, H. Dai, A. Thess, R. Lee, N. M. Hanjani, D. L. Dehaas, and R. E. Smalley, Phys. Rev. B **55**, R4921 (1997).

⁹ A. Bachtold *et al.*, Phys. Rev. Lett. **87**, 166801 (2001).

¹⁰ A. Yu. Kasumov *et al.*, Science **284**, 1508 (1999).

¹¹ A. F. Morpurgo *et al.*, Science **286**, 263 (1999).

¹² M. Kociak *et al.*, Phys. Rev. Lett. **86**, 2416 (2001). A. Kasumov *et al.*, Phys. Rev. B **68**, 214521 (2003).

¹³ Z. Tang *et al.*, Science **292**, 2462 (2001).

¹⁴ M. Kociak, *et al.*, Phys. Rev. Lett. **86**, 2416 (2001).

¹⁵ I. Takesue *et al.*, Phys. Rev. Lett. **96**, 057001 (2006).

¹⁶ S. Bellucci, M. Cini, P. Onorato, and E. Perfetto, J. Phys.: Condens. Matter **18**, S2115 (2006).

¹⁷ Enrico Perfetto and Michele Cini, Phys. Rev. B **69**, 092508 (2004)

¹⁸ J. González, and E. Perfetto, Phys. Rev. B **72**, 205406 (2005).

¹⁹ J. González and E. Perfetto, Eur. Phys. J. **51**, 571 (2006).

²⁰ The analysis of Ref.3 for a general interaction potential predicts that a crossover range of temperatures should be observable on temperature scales $T_f < T < T_b$, with a SC phase just corresponding to the regime $T < T_f$ dominated by the true $T = 0$ fixed point. For long-ranged interactions, we have $T_f \approx T_b$, and the intermediate regime is not observable. However in our case we assume a breakdown of the Luttinger regime below the highest of the two temperatures T_f and T_c .

²¹ Yu.A. Krotov, D.H. Lee, and S.G. Louie, Phys. Rev. Lett. **78**, 4245 (1997).

²² E. Perfetto, G. Stefanucci, and M. Cini Phys. Rev. B **66**, 165434 (2002).

²³ A. Balzarotti, M. Cini, E. Perfetto, and G. Stefanucci, J. Phys.: Condens. Matter **66**, 1387 (2004).

²⁴ W. Kohn, and J. M. Luttinger, Phys. Rev. Lett. **15**, 524 (1965).

²⁵ E. Perfetto, G. Stefanucci, and M. Cini, Eur. Phys. J.B **30**, 139 (2002).

²⁶ M. Cini, and A. D'Andrea, in Auger Spectroscopy and Electronic Structure, G. Cubotti, G. Mondio and K. Wandelt Editors, Springer Series in Surface Science , Springer-Verlag Berlin (1989)